Ultrasound in Med. & Biol., Vol. 40, No. 6, pp. 1037–1048, 2014

0301-5629/$ - see front matter

http://dx.doi.org/10.1016/j.ultrasmedbio.2014.01.008

● *Review*

INTRAVASCULAR PHOTOACOUSTIC IMAGING: A NEW TOOL FOR VULNERABLE PLAQUE IDENTIFICATION

Krista Jansen,*† Gijs van Soest,* and Antonius F. W. van der Steen*†‡

*Department of Biomedical Engineering, Thorax Centre, Erasmus University Medical Center, Rotterdam, The Netherlands; †Interuniversity Cardiology Institute of The Netherlands–Netherlands Heart Institute, Utrecht, The Netherlands; and ‡Department of Imaging Science and Technology, Delft University of Technology, Delft, The Netherlands

(*Received* 17 *September* 2013; *revised* 6 *January* 2014; *in final form* 7 *January* 2014)

Abstract—The vulnerable atherosclerotic plaque is believed to be at the root of the majority of acute coronary events. Even though the exact origins of plaque vulnerability remain elusive, the thin-cap fibroatheroma, characterized by a lipid-rich necrotic core covered by a thin fibrous cap, is considered to be the most prominent type of vulnerable plaque. No clinically available imaging technique can characterize atherosclerotic lesions to the extent needed to determine plaque vulnerability prognostically. Intravascular photoacoustic imaging (IVPA) has the potential to take a significant step in that direction by imaging both plaque structure and composition. IVPA is a natural extension of intravascular ultrasound that adds tissue type specificity to the images. IVPA utilizes the optical contrast provided by the differences in the absorption spectra of plaque components to image composition. Its capability to image lipids in human coronary atherosclerosis has been shown extensively *ex vivo* and has recently been translated to an *in vivo* animal model. Other disease markers that have been successfully targeted are calcium and inflammatory markers, such as macrophages and matrix metalloproteinase; the latter two through application of exogenous contrast agents. By simultaneously displaying plaque morphology and composition, IVPA can provide a powerful prognostic marker for disease progression, and as such has the potential to transform the current practice in percutaneous coronary intervention. (E-mail: g.vansoest@erasmusmc.nl)

Key Words: **Photoacoustic imaging, Intravascular ultrasound, Atherosclerosis, Vulnerable plaque, Tissue characterization.**

INTRODUCTION

The rupture of vulnerable atherosclerotic plaques is a major contributor to acute cardiovascular events and sudden cardiac deaths (Falk et al. 1995). In 2008, out of the 17.3 million cardiovascular deaths worldwide, heart attacks were responsible for 7.3 million deaths (World Health Organization 2008). The vulnerability of an atherosclerotic plaque, its susceptibility to rupture, is known to be related to the composition of the plaque, the distribution of mechanical stress within it, and the presence and extent of associated inflammation (Richardson et al. 1989; Schaar et al. 2004; Virmani et al. 2000). One of the most common types of vulnerable plaques is the thin-cap fibroatheroma. These lesions are characterized by a thin fibrous cap, weakened by the presence of macrophages, covering a lipid-rich necrotic core (Schaar et al. 2004). Rupture of the cap due to high mechanical stress will release the thrombogenic contents of the necrotic core into the bloodstream. The subsequent formation of a platelet-rich thrombus may result in occlusion, either at the location of the rupture or downstream from the lesion site. If this occlusion takes place in a coronary artery, the result may be unstable angina or a myocardial infarction. The key to plaque vulnerability is still elusive, even though recent advances in intravascular imaging technology have enabled the collection of a wealth of data on unstable atherosclerosis in all its stages of development (Waxman et al. 2006), both in clinical and in *ex vivo* settings. Plaque type and morphology are relevant for planning percutaneous coronary intervention and significantly affect long-term treatment outcome (Kolodgie et al. 2001).

The current standard for intravascular assessment of coronary atherosclerotic disease and guidance of interventional procedures is intra-vascular ultrasound (IVUS). This modality produces images based on the reflected

Address correspondence to: Gijs van Soest, Department of Biomedical Engineering, Thorax Centre, Erasmus MC, Ee23.02, PO Box 2040, 3000 CA Rotterdam, The Netherlands. E-mail: g.vansoest@erasmusmc.nl

amplitude of ultrasound pulses, providing information on both lumen geometry and the structure of the vascular wall with a resolution of approximately 100 μm and an imaging depth of 7 mm. IVUS is used in clinical practice and trials to measure lumen dimensions, degree of stenosis, plaque burden and to assess calcification and stent deployment.

As outlined above, plaque composition is a highly relevant parameter for its vulnerability. Technologies for imaging tissue type in the vessel wall are scant, however. The sensitivity and specificity of IVUS gray-scale for plaque composition is limited (de Korte et al. 2000) because the contrast between soft tissue types is minimal. IVUS radio frequency data analysis techniques for tissue characterization have been developed as an extension to gray-scale imaging (Nair et al. 2002). Today, two commercial IVUS systems offer coronary tissue characterization: VH-IVUS (20 MHz, phased-array transducer; Volcano Therapeutics, Rancho Cordova, CA, USA) and iMap (40 MHz, mechanical-type transducer; Boston Scientific, Fremont, CA, USA). VH-IVUS differentiates four tissue types: necrotic core, fibrous, fibrofatty and dense calcium (Garcia-Garcia et al. 2010) but has shown limited accuracy in complex lesions in a porcine model (Granada et al. 2007; Thim et al. 2010). iMap distinguishes similar tissue types: fibrotic, lipidic, necrotic and calcified tissue. An *in vivo* comparison between VH-IVUS and iMap yielded a significant and systematic variability in plaque composition estimates (Shin et al. 2011). These conflicting observations have fueled an ongoing debate about the appropriate interpretation of ultrasound-based tissue characterization.

Intravascular optical coherence tomography (IVOCT) is another modality based on the echo delay of light backscattered from the tissue. IVOCT provides high resolution images (15 μm) but with limited depth penetration (1–2 mm) (Tearney et al. 2008). Flushing of the artery under inspection is required due to the strong signal attenuation through blood. Widespread clinical acceptance was achieved after the introduction of high frame rate (>100 frames per s) and pullback speed (20–40 mm/s). Compared to IVUS, optical coherence tomography (OCT) offers better assessment of lumen geometry, fibrous cap thickness, stent structure, stent strut coverage and detection of macrophages (Tearney et al. 2003, 2012). On the other hand, tissue characterization by IVOCT is less straightforward and is currently a topic of intense research (van Soest et al. 2010).

In the past decade, a number of other optical technologies have aimed to improve intra-vascular tissue characterization. The most advanced in terms of clinical penetration is near-infrared reflection spectroscopy (NIRS), which is developed and commercialized by Infraredx Inc. (Burlington, MA, USA). It collects a reflection spectrum of the arterial wall, through blood, and identifies the presence of lipid-core plaque in the artery wall. Recently, our laboratory collaborated with Infraredx to develop a hybrid NIRS/IVUS catheter that combines morphologic imaging and lipid detection (Gardner et al. 2008; Garg et al. 2010; Moreno et al. 2002). This is the first multi-modality device to enter the clinical arena (TVC, Infraredx). Combined interpretation of IVUS and NIRS data may yield an assessment of the lesion morphology. This also highlights a limitation of NIRS: it is not an imaging modality. Because it lacks depth resolution, NIRS can identify the presence but not the amount or the location, relative to the lumen, of the lipid core. The sensing depth of NIRS is not well quantified.

Intravascular photoacoustics (IVPA) is the most recent addition to spectroscopic diagnostic techniques and is the topic of this review. IVPA has the ability to directly image tissue components in the vessel wall, with high chemical specificity for lipid type. There is potential to extend the technology to identify other factors such as dense macrophage infiltration, associated with plaque vulnerability. The same catheter can be used simultaneously to image the arterial wall architecture by IVUS. A review by Wang et al. (2010b) laid out the basics of IVPA; we focus here on developments that have emerged since that work appeared.

Principle of photoacoustics

In photoacoustic (PA) imaging, the tissue is irradiated by short laser pulses with a length of several nanoseconds. Absorption of laser light transfers the optical energy to the tissue, which causes a transient pressure rise (Oraevsky and Karabutov 2003). This initial pressure rise acts as an acoustic source that generates a broadband wave propagating through the tissue. The acoustic wave can be detected with an ultrasound transducer. An image can be created by scanning either the ultrasound or the optical beam and deriving depth resolution from the time-of-flight of the ultrasound wave. Note that the time-of-flight is one-way only because the propagation delay of light is negligible. The prime advantage of such an ultrasound-mediated image, generated by an optical contrast mechanism, is that it provides the advantages of both resolution and viewing depth of ultrasound and chemical specificity of optical absorption.

In IVPA, this principle needs to be miniaturized to fit on a catheter. Light is delivered through an optical fiber, while signal detection is performed by the same type of ultrasound transducer that is used in IVUS. The arrangement of fiber and transducer must be such, that the tissue within the field of view of the transducer is illuminated. The small, unfocused single-element devices used in IVUS offer the opportunity to create small catheters. The principle of IVPA is shown in Figure 1.

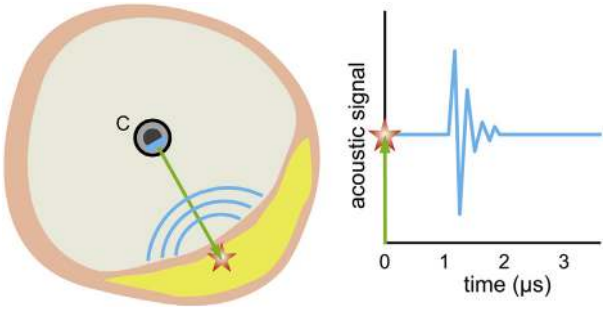

Fig. 1. Sketch of the intravascular photoacoustic imaging (IVPA) principle. A laser pulse (green) is sent from the catheter (C) to the vessel wall containing a plaque (yellow). The light excites an acoustic wave (blue curves) through optical absorption and the associated thermoelastic expansion (red star). The graph on the right shows a time trace of the acoustic signal after the laser fires at time $t = 0$.

The PA source strength p_0 is described by the relation $p_0 = \Gamma \mu_a F$, where F is the optical energy density, μ_a is the absorption coefficient and $\Gamma = \beta c_0^2/C_p$ is the Grüneisen parameter. This number describes the thermo-acoustic conversion efficiency and depends on the thermal expansion coefficient β, the acoustic wave velocity c_0, and the specific heat at constant pressure C_p. The variation of the absorption coefficient with the excitation wavelength is the tissue-specific chemical absorption spectrum, which permits differentiation of tissue type (Fig. 2). The PA excitation wavelengths can be selected to give maximum absorption contrast between the relevant components in the vessel wall and plaque, such as collagen, calcified tissue, and lipids (Tromberg et al. 2000; Van Veen et al. 2004), to image plaque

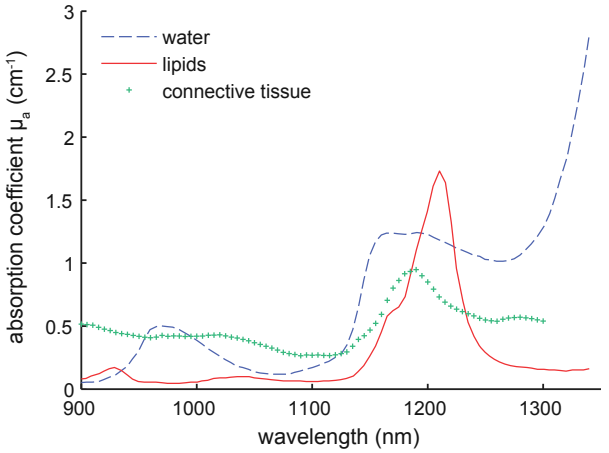

Fig. 2. Absorption spectra of various absorbers present in coronary artery vessel wall. Water, fat, and connective tissue (collagen and elastin) are the major contributors to the absorption spectra of human tissues in the near-infrared spectral region (Tsai et al. 2001).

composition using endogenous contrast. Alternatively, exogenous absorbers can be utilized to generate contrast for vulnerable plaque markers that would otherwise remain invisible due to their relatively featureless or low-amplitude absorption spectra. Macrophages are an example of such plaque components. Conventional PA imaging often relies on blood as a chromophore, which is a much more strongly absorbing tissue than typical vessel wall components. Hence, the signal strength in IVPA is generally small and transducer sensitivity is an important requirement.

Development of IVPA

Endogenous contrast: imaging of lipids and calcification. The goal of IVPA imaging is the chemical characterization of vessel wall components. Historically, development has been driven by the availability of suitable light sources. For this reason, the first spectroscopic measurements focused on the visible wavelength range (410–680 nm) (Al Dhahir et al. 1990; Prince et al. 1986). Through PA imaging of human atherosclerotic aorta specimens, contrast for lipids was found at 461 and 532 nm (Beard and Mills 1997) and contrast for calcium at 308 nm (Crazzolara et al. 1991). Discrimination between normal and atheromatous areas of arterial tissue in the visible range has an important drawback, at these wavelengths blood (hemoglobin) absorption is also very high. Introduction of infrared sources prompted investigation of a wider range of excitation wavelengths (680–1800 nm). Blood absorption is especially low in the wavelength range from 680–1300 nm. In this wavelength range, the absorption spectrum of lipids exhibits a large peak around 1210 nm (Fig. 2). The group led by Emelianov, pioneered spectroscopic IVPA to distinguish between lipid-rich tissue and collagen (Sethuraman et al. 2008). They performed imaging of ex vivo normal and atherosclerotic rabbit aorta samples using a bench-top setup with a commercial IVUS catheter and external illumination. They found different spectral slopes in the IVPA image in regions identified as lipid-rich collagen type I and collagen type III. The same group subsequently exploited the absorption peak around 1210 nm to image lipids in atherosclerotic rabbit aorta (Wang et al. 2010a).

Allen and Beard (2009) were the first to exploit the low blood absorption in the near infrared to discriminate between lipid-rich and normal vascular tissue while imaging through several millimeters of blood (Allen et al. 2012). Imaging through blood is difficult because of the strong attenuation of the excitation light. They investigated samples of atherosclerotic human aorta and confirmed the presence of lipids by comparing the PA spectra obtained in a region within the plaque to the spectral signature of a lump of fat.

Investigation of PA response at longer wavelengths yielded an additional lipid specific absorption feature around 1720 nm (Allen and Beard 2009). Bo Wang et al. (2012b) imaged an atherosclerotic rabbit aorta *ex vivo* in the presence of luminal blood using excitation light at that wavelength. They demonstrated single wavelength IVPA imaging of lipids through blood using relatively low laser output energy. However, the specificity of this single wavelength method for lipids in human atherosclerotic plaques remains to be investigated.

The first demonstration of *in vivo* IVPA was performed using the same 1720 nm single wavelength in a hypercholesterolemic rabbit model (Wang et al. 2012a), see Figure 3. The study was limited by the slow laser system, which necessitated a complex breath gating acquisition. It did show, however, that *in vivo* imaging without flushing the blood from the artery is possible.

In most IVPA experiments, lipid rich atherosclerotic plaques were distinguished from normal arterial tissue by simply comparing the tissue spectral signature to the absorption spectra of lipids. A more sophisticated spectroscopy inversion approach could provide robust identification of a wider range of tissue types, including collagen, elastin and calcifications. Pu Wang et al. (2012c) recorded spectroscopic PA data of a phantom consisting of rat-tail tendon and fat between 1650–1850 nm. A multi-variate curve fit analysis yielded the spatial distribution of collagen and lipids in the phantom.

Photoacoustic generation is temperature dependent, and the dependence is tissue specific, which provides another contrast mechanism. With increasing tissue temperature, the PA amplitude of atherosclerotic plaque lipids decreased while the PA amplitude of peri-adventitial lipids and abdominal fat remained relatively constant between 20–38°C (Wang and Emelianov 2011). Thermal IVPA imaging of atherosclerotic lipids has the advantage over spectroscopic IVPA that only one wavelength is needed. However, creating reliable temperature differences *in vivo* might prove difficult.

IVPA imaging of human coronary atherosclerosis. In 2011, we reported the first IVPA imaging of human atherosclerotic coronary arteries ex vivo (Jansen et al. 2011). Specific imaging of lipids was shown by spectroscopic imaging over the wavelength range 715–1400 nm, making use of the peak in the lipid absorption spectrum around 1210 nm. This distinct peak was used to differentiate lipids from other tissue components of the vessel wall. In contrast to earlier work, an actual prototype IVPA catheter, with intra-vascular illumination of tissue, was used to image the arteries. Fresh human coronary arteries, showing different stages of disease, were imaged ex vivo by co-registered IVPA/IVUS. A result is shown in Figure 4 (a). The histology shows circumferential intimal thickening with a large eccentric lipid-rich lesion, as well as a calcified area and regions of peri-adventitial fat. The IVUS data confirms this morphology. The IVPA image at 1210 nm exhibits a bright signal along the intimal border, as well as from deeper tissue layers in the eccentric plaque and the peri-adventitial fat in the bottom right corner. At 1230 nm, the signal in these regions is markedly lower, in accordance with the absorption spectrum of lipids in this wavelength range. Collocated with the enhanced 1210 nm IVPA signal a positive Oil Red O stain is observed, particularly in the plaque, indicating the presence of lipids. Since the variation in the laser pulse energy and tissue scattering properties is negligible over the wavelength range 1210–1230 nm, the light fluence at every location could be assumed equal. Photoacoustic spectra were acquired along image lines sampling the plaque tissue. In Figure 4 (b), the spectra at three locations are shown, two inside the

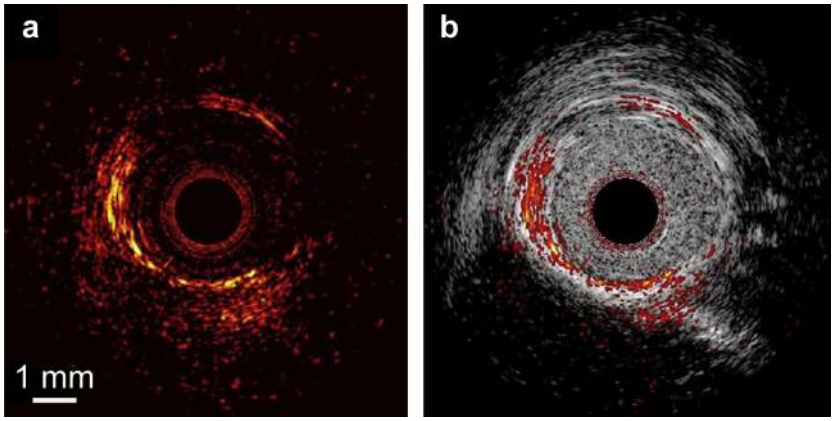

Fig. 3. In vivo IVPA/intravascular ultrasound (IVUS) imaging of lipid in an abdominal rabbit aorta. (a) IVPA image and (b) combined IVPA/IVUS image. The location of lipid deposits in the vessel wall is visualized in the combined IVPA/IVUS image. Adapted from Wang et al. (2012a).

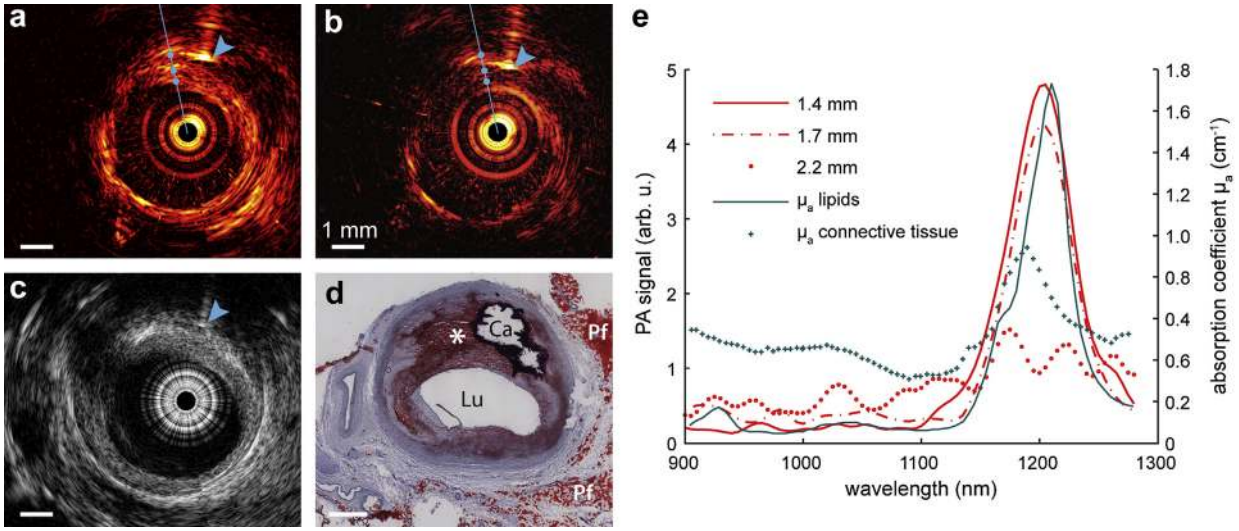

Fig. 4. IVPA/IVUS imaging of an advanced human atherosclerotic plaque. IVPA images at (a) 1210 nm (high lipid absorption) and (b) 1230 nm (low lipid absorption). (c) IVUS image. Full spectral scans were made along the blue line in (a) and (b). Arrowheads indicate the needle used for marking. (d) Histology: Oil Red O stain shows the presence of a lipid-rich plaque (*) as well as a calcified area (Ca). Lu, lumen; Pf, peri-adventitial fat. (e) Photoacoustic spectra at three locations on the blue line in (a) and (b), indicated by the blue dots. The sites at 1.4- and 1.7-mm distance from the catheter are located within the lipid-rich plaque. The corresponding photoacoustic (PA) spectra show strong resemblance to the lipid absorption reference. The site at 2.2 mm is located just outside the plaque area. Adapted from Jansen et al. (2011).

lipid-rich plaque region and one just outside. The absorption spectra of lipids and connective tissue (Tsai et al. 2001) are included for reference. The two spectra located in the plaque clearly match the lipid reference, while the third lacks the pronounced peak.

Automatic spectroscopic IVPA detection of lipids (Fig. 5) can be achieved using the same catheter and experimental setup. Co-registered cross-sectional IVPA/IVUS scans of fresh *ex vivo* human coronary arteries from 1185–1235 nm at 10 nm intervals were acquired. For each pixel in the resulting data set, we computed the correlation of the IVPA spectra with a reference lipid absorption spectrum. The lipid matching regions—those with a correlation coefficient equal to or higher than an empirically chosen threshold—exhibited good correspondence with the histologic lipid stain of the same cross section (Fig. 5c and d). These experiments provide proof of principle for robust IVPA imaging of plaque composition with as few as three different wavelengths (Jansen et al. 2013).

IVPA imaging at 1720 nm was also demonstrated on human coronary atherosclerosis *ex vivo* (Wang et al. 2012a). Working at a single wavelength has advantages of speed and simplicity of the laser source but risks losing chemical specificity. We recently compared the 1.2 μm and 1.7 μm wavelength bands and found that both are suitable for imaging lipids in atherosclerosis (Jansen et al. 2014). The chemical specificity of either wavelength range, as well as the potential for imaging with few wavelengths needs to be confirmed in more elaborate studies.

Exogenous contrast: imaging of macrophages and matrix metalloproteinase. Vulnerable plaque markers that lack sufficient endogenous contrast can be imaged using exogenous absorbers. Macrophages are an example of such plaque components. They do not provide endogenous contrast but can be visualized using gold nanoparticles. The gold nanoparticles have a distinct absorption peak in the visible wavelength range. When the nanoparticles are endocytosed by macrophages, they aggregate. These aggregated gold nanoparticles have a shifted peak in the absorption spectrum compared to the (extracellular) non-aggregated gold nanoparticles, providing image contrast. This principle was proven in an atherosclerotic rabbit aorta injected with macrophages loaded with gold nanoparticles in a bench-top experimental setting (Wang et al. 2009). The resulting IVPA images, shown in Figure 6, demonstrate that the aggregated gold nanoparticles produce the strongest PA signal at 700 nm wavelength. The extravasation of nanoparticles in atherosclerotic regions with compromised luminal endothelium and acute inflammation was shown by systemic injection of gold nanoparticles in a live rabbit model, followed by *ex vivo* IVPA imaging (Yeager et al. 2012). IVPA/IVUS imaging at 750 nm revealed a high PA signal from localized gold nanoparticles in regions with atherosclerotic plaques.

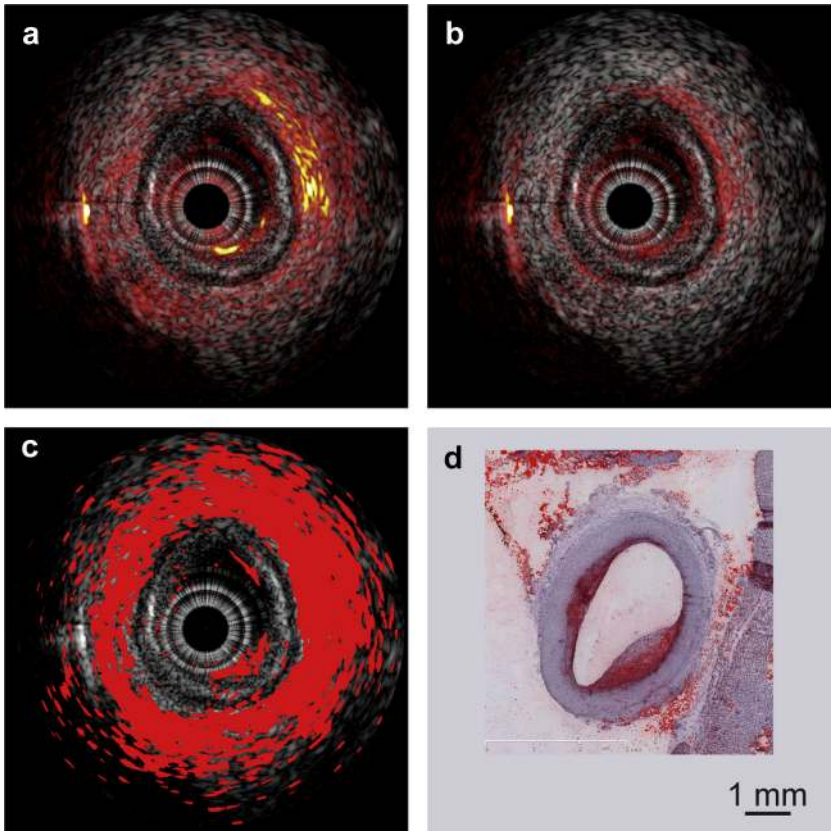

Fig. 5. Combined IVPA/IVUS images at (a) 1205 nm and (b) 1235 nm of a human coronary artery with low-grade disease. (c) Automatic lipid detection image overlaid on IVUS image. (d) Lipid histology stain (ORO). Adapted from Jansen et al. (2013).

Matrix metalloproteinase (MMP) activity, an indicator of plaque instability, can be detected using a MMP-activatable fluorescent imaging agent. MMPSense (MMPSense 680; VisEn Medical, Boston, MA, USA) is such an imaging agent and is activated by different enzymes, most prominently MMP2/9 and trypsin, and to a lesser extent by other proteases. Once activated, it becomes optically absorbing. More than 80% of the absorbed energy is transferred into PA signals, due to the low quantum yield of the dye. It has a much lower absorption than gold nanoparticles and thus produces a much lower PA signal intensity.

MMPSense was used for detecting MMP activity in human carotid arteries (Razansky et al. 2012). Immediately after endarterectomy, the atherosclerotic specimens were incubated in MMPSense. The morphologic PA images, shown in Figure 7 (a, c, e), were obtained using a small-animal imaging system. The activated probe was distinguished from the background and the inactive probe, by acquiring PA data at several wavelengths and analyzing spectral contributions on a per-pixel basis. The results matched well with fluorescence microscopy (Fig. 7b, d, f).

IVPA catheter development

Practical *in vivo* implementation of IVPA requires the development of a dedicated catheter device. Such a device needs to incorporate an optical axis to deliver the light to the vessel wall and an ultrasound detector to detect the PA signals. Various designs have been proposed.

A miniature, all-optical IVPA probe based on a Fabry-Perot ultrasound sensor was built (Zhang and Beard 2011). It had a diameter of only 250 μm and exhibited good acoustic sensitivity. This all-optical design of an IVPA imaging probe lacks IVUS functionality but has the potential for multi-modal operation and could be combined with OCT and other optical imaging and sensing methods.

Devices that contain a piezoelectric ultrasound transducer for detection of PA signals can be used for combined IVPA/IVUS imaging to provide simultaneous information on composition and morphology of the arterial wall. Two early prototype catheters combined an optical fiber for light delivery with a commercially available IVUS imaging catheter (Atlantis SR plus, Boston Scientific, Inc.) for both pulse-echo ultrasound imaging and detection of PA signals (Karpiouk et al. 2010). Light

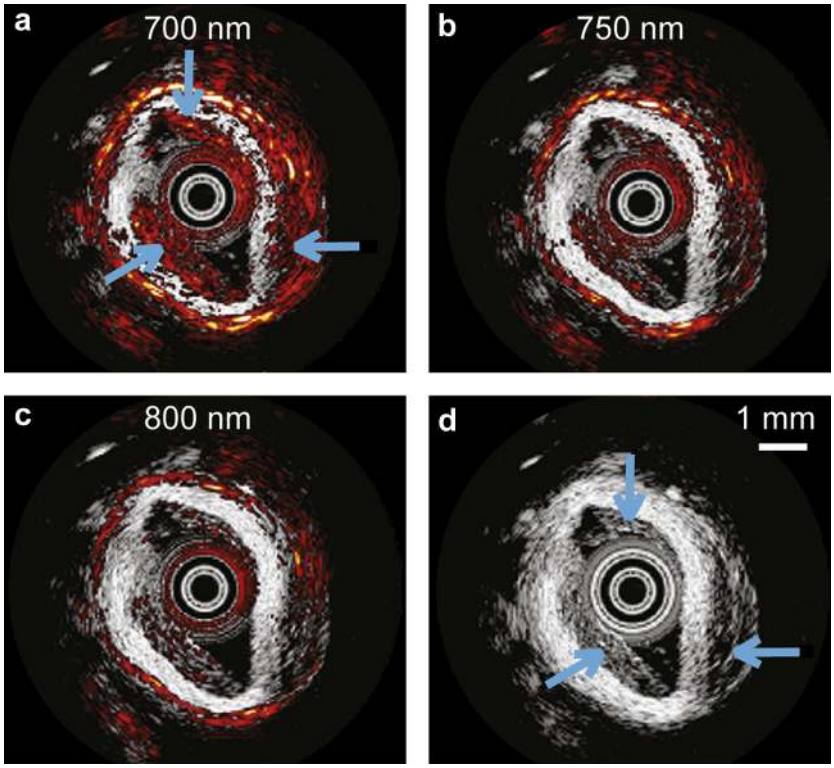

Fig. 6. Combined IVPA/IVUS images at 700, 750 and 800 nm (a-c) and IVUS image (d) of a diseased rabbit aorta injected with macrophages loaded with gold nanoparticles (blue arrows). The combined IVPA/IVUS images taken at 700 nm wavelength (a) showed high photoacoustic signal at the injected regions denoted by arrows. Adapted from Wang et al. (2009).

was directed toward the vessel wall using an angle-polished fiber ("side-fire fiber") or a silver-coated glass mirror.

A step toward an array catheter for PA imaging analogous to Volcano's electronic IVUS catheter was made (Hsieh et al. 2010). When using omni-directional optical excitation and ultrasound transmission and detection, no rotation is needed and the required laser pulse repetition rate is reduced. A prototype of a catheter with omni-directional light delivery consisted of a multi-mode optical fiber coupled to a cone-shaped mirror for illumination and an optical ultrasound detector. The outer diameter of the device was 3 mm.

Early integrated IVPA catheters were too large to use in human coronary arteries, and have only been tested on phantoms, rabbit aortas and human arteries that were opened up to enable *en-face* scanning of the luminal surface. Recently, we achieved a vital step toward miniaturization of IVPA devices by building a hybrid IVPA/IVUS catheter with an outer diameter of 1.25 mm. The catheter consisted of a 400-μm diameter core optical fiber and an IVUS transducer with a diameter of 1.0 mm (Jansen et al. 2010). A schematic illustration and a photograph of the catheter tip are shown in Figure 8 (a and b), respectively. The tip of the fiber was polished at an angle of 34° and covered with a glued-on quartz cap to preserve an air-glass interface deflecting the beam by total reflection. The transducer had a wide frequency bandwidth centered at 30 MHz. The fiber and the transducer were mounted in a tip assembly (Fig. 8b). Using this probe, we imaged intact human coronary arteries *ex vivo* (Jansen et al. 2011).

A variation on this design used a side-firing optical fiber and side-viewing ultrasonic transducer arranged side-by-side (Li et al. 2012). The fiber and transducer were packaged in polyimide tubing with an outer diameter of 1.2 mm; making it the smallest catheter to date that combines IVPA and IVUS imaging. The arrangement of the fiber and transducer minimizes the offset of the beams, which may improve the optical–acoustic overlapping, especially close to the probe.

The probes described previously all derive their transverse imaging resolution from the acoustic beam properties: light is assumed to be diffuse and excite a PA signal throughout a large area, part of which is sampled by the acoustic beam. Optical-resolution PA imaging (Maslov et al. 2008) provides better transverse resolution, as light can be focused to a smaller diameter than

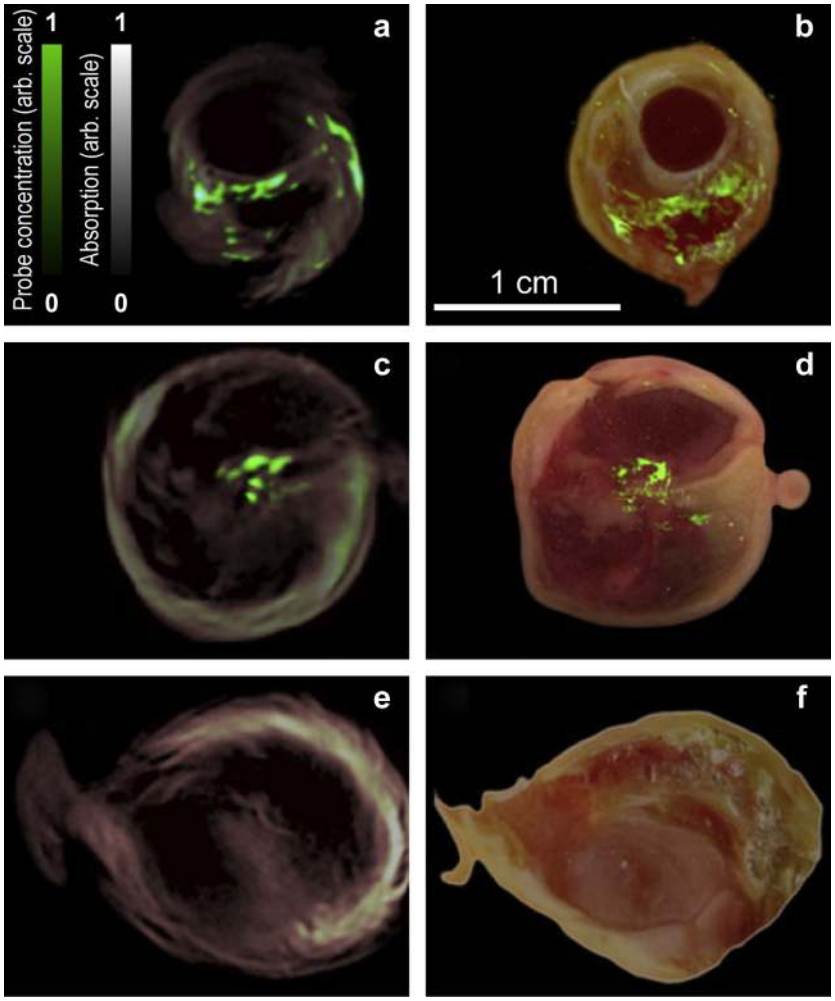

Fig. 7. Localization of matrix metalloproteinase (MMP) activity in three carotid specimens. Samples 1 (top row) and 2 (middle row) were incubated in MMPSense 680 while sample 3 (bottom row) was incubated in PBS. (a), (c) and (e): PA imaging results of intact plaques. Cross-sectional spectroscopic reconstruction, revealing location of MMPSense 680 activity in the slice, is shown in green color that is superimposed onto morphologic photoacoustic images. (b), (d) and (f): The corresponding epi-fluorescent images from dissected plaque (in green) superimposed onto color images of cryosections from the three carotid plaque specimen. Adapted from Razansky et al. (2012).

ultrasound at diagnostic frequencies. The resolution advantage comes at the cost of viewing depth, which is necessary to create cross-sectional images. This limits the use of optical-resolution approaches for intravascular imaging.

DISCUSSION

IVPA is an experimental technique that is currently being developed in *ex vivo* experiments, undergoing continuous further refinement. Although it has shown the ability to fill an important niche, many facets of real-time clinical imaging still need to be resolved. Several important aspects of the optimal image acquisition sequence, laser sources, catheter design, *etc.*, are currently under investigation. The road to *in vivo* IVPA imaging will present some specific challenges that we discuss below.

In order to obtain optimal PA signal strength, it is desirable to deliver as much light to the vessel wall as possible within the physical boundaries of the instrument and within the safety limits. Blood is a strongly scattering tissue, which can markedly reduce the light intensity at the vessel wall, even at wavelengths in the near infrared region. Several *ex vivo* IVPA experiments have shown IVPA imaging through blood (Allen and Beard 2009; Allen et al. 2012; Wang et al. 2012a, 2012b) but the image quality deteriorates considerably in the presence of luminal blood. Even when imaging at 1720 nm, at very high lipid absorption, the image quality and

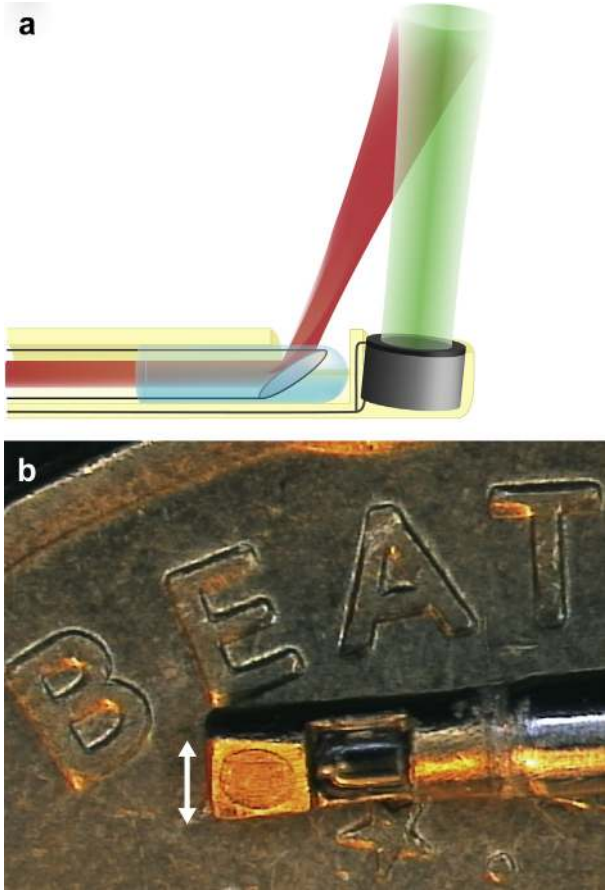

Fig. 8. (a) Detailed schematic of the catheter tip of a combined IVUS/IVPA catheter, showing the beam layout (light beam in red; US beam in green). (b) Photograph of the catheter tip on the edge of a 10 eurocent coin. The outer diameter of the catheter tip is 1.25 mm (white arrows). Adapted from Jansen et al. (2011).

reliability of the atherosclerotic lipid detection by IVPA would be greatly improved by flushing. It therefore appears likely that IVPA imaging may involve flushing of the blood from the artery in the clinical setting. Blood clearing is standard practice in IVOCT imaging. Unlike IVOCT, IVPA does not rely on the complete suppression of scattering in the lumen, but only requires the delivery of sufficient power. This means that dilution, rather than complete clearing, may be good enough. On the other hand, the ultrasonic properties of the flush media used for OCT (iodixanol, a coronary angiography contrast agent, trade name Visipaque (GE Healthcare, Princeton, NJ, USA)) are not precisely known, so investigation of alternatives may be needed.

IVPA poses a set of strict requirements on the light source. Lasers used in development of the technology are powerful and versatile, but slow at pulse repetition rates of 10–50 Hz. This low pulse frequency precludes *in vivo* imaging. Particularly if flushing is used, the optimal imaging sequence will be modeled on that of Fourier domain OCT: high frame rate, high pullback speed, short pullback time of <10 s. This acquisition protocol prescribes a light source with a repetition rate of the order of 10 kHz, with wavelengths that generate relevant contrast. Such lasers are currently being developed (Li et al. 2013).

The smallest combined IVPA/IVUS catheter diameter built to date has a diameter of 1.2 mm. Current IVUS probes have an outer diameter of less than 1 mm, including the protective sheath in which they rotate. Future developments will reduce the IVPA catheter diameter to 1 mm or less for successful application in clinical practice. All-optical devices are much smaller but sacrifice IVUS functionality. As in ultrasound imaging, both bandwidth (for axial resolution) and sensitivity are important parameters for transducer selection. The small signal strength in IVPA means that sensitivity should be considered the more critical of the two. Most devices demonstrated to date work in the frequency range that is also used for IVUS. There is no experimental data to support that this range is actually optimal. Further optimization of transducers needs to be part of the effort to bring IVPA to clinical applicability.

IVPA is undergoing rapid development to become a clinically viable technology. Table 1 gives an overview of the advantages and disadvantages of the different intravascular imaging modalities and their capacity to detect the different markers of plaque vulnerability. There is no single technique that can determine plaque vulnerability completely, which is why multi-modality imaging is frequently proposed. IVPA can differentiate between plaque components by using the differences in the optical absorption spectra of different tissues, like NIRS. However, unlike NIRS, it has depth resolution, which makes it possible to know the exact spatial location of the lipids relative to the lumen border. IVPA provides optical contrast with ultrasound imaging depth. If used in combination with IVUS, IVPA can provide information on plaque composition that complements the morphologic information provided by IVUS. In the future, useful combinations with other imaging modalities are likely to be explored such as an IVPA/OCT combination.

IVPA can potentially become a very powerful tool for guidance of percutaneous coronary intervention, informing the decision of which plaque to treat and length to stent with detailed composition information. The occurrence of incomplete stent coverage of lipid-rich plaques, despite adequate coverage of the angiographic stenosis, demonstrates the limitations of standard angiography to delineate the borders of the plaque. Incomplete stent coverage can potentially cause lipid-rich plaque disruption during stent placement, which can result in distal embolization (Schultz et al. 2010). Incomplete stent

Table 1. Intravascular imaging modalities: strengths and weaknesses compared

	Grayscale IVUS	VH-IVUS/iMap	Palpography	NIRS	IVOCT	IVPA
Image	Cross-section structure	Cross-section tissue type	Radial strain map (elastogram)	Lipid-core plaque map (chemogram)	Cross-section structure	Cross-section tissue type
Type of radiation	Ultrasound	Ultrasound	Ultrasound	Near-IR light	Near-IR light	(Near-IR) light + ultrasound
Axial resolution (μm)	100–200	>250	450	N/A	10–15	100
Lateral resolution (μm)	300–500	300–500	300–500	1000	30–40	400–500
Penetration (mm)	10	5	N/A	unknown	1	5
Contrast mechanism	Acoustic scattering	Acoustic Spectrum	Tissue strain	Optical absorption	Optical scattering	Optical absorption
Pullback rate	0.5 mm/s	0.5 mm/s	0.5 mm/s	0.5 mm/s	20–40 mm/s	N/A*
Flushing	no	No	no	no	Yes	TBD†
Current status	CS/CA	CS/CA	CS	CS/CA	CS/CA	PCS
Lumen area	++	++	−	−	++	±
Plaque burden	++	++	−	−	−	±
Positive remodeling	++	++	−	−	−	±
Necrotic core	±	++	++	++	−	++
Fibrous-cap thickness	−	−	−	−	+	−
TCFA‡	−	±	++	−	+	±?
Plaque rupture	+	+	−	−	++	−
Erosion	−	−	−	−	+	−
Thrombus	±	±	−	−	+	−
Inflammation	−	−	−	−	±	±?
Calcium	++	++	++	−	+	−

IVUS = intravascular ultrasound; VH = virtual histology; NIRS = near-infrared spectroscopy; IVOCT = intravascular optical coherence tomography; NIRF = near-infrared fluorescence; IVPA = intravascular photoacoustics; CA = clinically, commercially available; CS = clinical studies; PCS = pre-clinical studies; N/A = not applicable; TBD = to be determined; TCFA = thin-cap fibroatheroma.

++excellent.

+good.

±possible.

−impossible.

Data derived from Kubo and Akasaka (2012), Suh et al. (2011), MacNeill et al. (2003) and Maehara et al. (2009). Palpography data derived from Schaar et al. (2006).

*Current experimental IVPA/IVUS imaging systems are using a 10-Hz repetition rate laser. Pullback rate is calculated for using four wavelengths, 300 A-scans per slice and a step size of 200 μm.

† May not be required in specific wavelength bands (*e.g.,* the near-infrared window).

‡ The positive predictive value to detect "definite TCFA" (defined as agreement by both OCT and VH-IVUS) was 78% by OCT but only 46% by VH-IVUS by Sawada et al. (2008).

coverage is also suspected to be associated with plaque progression leading to stent failure due to edge restenosis (Waxman et al. 2010). IVPA will also contribute to studies of plaque vulnerability and allows quantification of the response to different forms of intervention (device, pharmacologic, lifestyle changes) with high chemical detail *in vivo*. IVPA could provide an imaging endpoint in clinical studies to show changes in the lipid content of atherosclerotic plaques (Serruys et al. 2008; Van Mieghem et al. 2006).

Acknowledgments—This work was funded by the Dutch Technology Foundation (STW) through the 2007 Simon Stevin Meester grant (STW 10040).

REFERENCES

Allen TJ, Beard PC. Photoacoustic characterisation of vascular tissue at NIR wavelengths. Photons Plus Ultrasound: Imaging and Sensing. San Jose, CA, USA: SPIE; 2009. 71770A–9.

Al Dhahir RK, Dyer PE, Zhu Z. Photoacoustic studies and selective ablation of vascular tissue using a pulsed dye laser. Appl Phys B 1990;51:81–85.

Allen TJ, Hall A, Dhillon AP, Owen JS, Beard PC. Spectroscopic photoacoustic imaging of lipid-rich plaques in the human aorta in the 740 to 1400 nm wavelength range. J Biomed Opt 2012;17:061209.

Beard PC, Mills TN. Characterization of post mortem arterial tissue using time-resolved photoacoustic spectroscopy at 436, 461 and 532 nm. Phys Med Biol 1997;42:177–198.

Crazzolara H, Vonmuench W, Rose C, Thiemann U, Haase KK, Ritter M, Karsch KR. Analysis of the acoustic response of vascular tissue irradiated by an ultraviolet-laser pulse. J Appl Phys 1991;70:1847–1849.

de Korte CL, Pasterkamp G, van der Steen AF, Woutman HA, Bom N. Characterization of plaque components with intravascular ultrasound elastography in human femoral and coronary arteries *in vitro*. Circulation 2000;102:617–623.

Falk E, Shah PK, Fuster V. Coronary plaque disruption. Circulation 1995;92:657–671.

Garcia-Garcia HM, Costa MA, Serruys PW. Imaging of coronary atherosclerosis: Intravascular ultrasound. Eur Heart J 2010;31:2456–2469.

Gardner CM, Tan H, Hull EL, Lisauskas JB, Sum ST, Meese TM, Jiang C, Madden SP, Caplan JD, Burke AP, Virmani R, Goldstein J, Muller JE. Detection of lipid core coronary plaques in autopsy specimens with a novel catheter-based near-infrared spectroscopy system. JACC Cardiovasc Imaging 2008;1:638–648.

Garg S, Serruys PW, van der Ent M, Schultz C, Mastik F, van Soest G, van der Steen AF, Wilder MA, Muller JE, Regar E. First use in patients of a combined near infra-red spectroscopy and intra-vascular ultrasound catheter to identify composition and structure of coronary plaque. EuroIntervention 2010;5:755–756.

Granada JF, Wallace-Bradley D, Win HK, Alviar CL, Builes A, Lev EI, Barrios R, Schulz DG, Raizner AE, Kaluza GL. *In vivo* plaque characterization using intravascular ultrasound-virtual histology in a porcine model of complex coronary lesions. Arterioscl Throm Vas 2007;27:387–393.

Hsieh BY, Chen SL, Ling T, Guo LJ, Li PC. Integrated intravascular ultrasound and photoacoustic imaging scan head. Opt Lett 2010;35:2892–2894.

Jansen K, Springeling G, Lancee C, Beurskens R, Mastik F, van der Steen AFW, van Soest G. An intravascular photoacoustic imaging catheter. In: International Ultrasonics Symposium (IUS), 2010 IEEE, San Diego, CA, USA. 2010;378–381.

Jansen K, van der Steen AFW, van Beusekom HMM, Oosterhuis JW, van Soest G. Intravascular photoacoustic imaging of human coronary atherosclerosis. Opt Lett 2011;36:597–599.

Jansen K, Wu M, van der Steen AFW, van Soest G. Lipid detection in atherosclerotic human coronaries by spectroscopic intravascular photoacoustic imaging. Opt Express 2013;21:21472–21484.

Jansen K, Wu M, van der Steen AFW, van Soest G. Photoacoustic imaging of human coronary atherosclerosis in two spectral bands. Photoacoustics 2014;2:12–20.

Karpiouk AB, Wang B, Emelianov SY. Development of a catheter for combined intravascular ultrasound and photoacoustic imaging. Rev Sci Instrum 2010;81:014901.

Kolodgie FD, Burke AP, Farb A, Gold HK, Yuan JY, Narula J, Finn AV, Virmani R. The thin-cap fibroatheroma: A type of vulnerable plaque: The major precursor lesion to acute coronary syndromes. Curr Opin Cardiol 2001;16:285–292.

Kubo T, Akasaka T. What is the optimal imaging tool for coronary atherosclerosis?. In: Arampatzis C, McFadden EP, Michalis LK, Virmani R, Serruys PW, (eds). Coronary atherosclerosis: current management and treatment. London, UK: Informa Healthcare; 2012.

Li R, Slipchenko MN, Wang P, Cheng J-X. Compact high power barium nitrite crystal-based Raman laser at 1197 nm for photoacoustic imaging of fat. J Biomed Opt 2013;18:040502.

Li X, Wei W, Zhou Q, Shung KK, Chen Z. Intravascular photoacoustic imaging at 35 and 80 MHz. J Biomed Opt 2012;17:106005.

MacNeill BD, Lowe HC, Takano M, Fuster V, Jang IK. Intravascular modalities for detection of vulnerable plaque: Current status. Arterioscl Throm Vas 2003;23:1333–1342.

Maehara A, Mintz GS, Weissman NJ. Advances in intravascular imaging. Circ Cardiovasc Interv 2009;2:482–490.

Maslov K, Zhang HF, Hu S, Wang LV. Optical-resolution photoacoustic microscopy for in vivo imaging of single capillaries. Opt Lett 2008;33:929–931.

Moreno PR, Lodder RA, Purushothaman KR, Charash WE, O'Connor WN, Muller JE. Detection of lipid pool, thin fibrous cap, and inflammatory cells in human aortic atherosclerotic plaques by near-infrared spectroscopy. Circulation 2002;105:923–927.

Nair A, Kuban BD, Tuzcu EM, Schoenhagen P, Nissen SE, Vince DG. Coronary plaque classification with intravascular ultrasound radiofrequency data analysis. Circulation 2002;106:2200–2206.

Oraevsky AA, Karabutov AA. Optoacoustic tomography. In: Vo-Dinh T, (ed). Biomedical Photonics Handbook. Boca Raton, FL: CRC Press; 2003.

Prince MR, Deutsch TF, Mathews-Roth MM, Margolis R, Parrish JA, Oseroff AR. Preferential light absorption in atheromas in vitro. Implications for laser angioplasty. J Clin Invest 1986;78:295–302.

Razansky D, Harlaar NJ, Hillebrands JL, Taruttis A, Herzog E, Zeebregts CJ, van Dam GM, Ntziachristos V. Multispectral optoacoustic tomography of matrix metalloproteinase activity in vulnerable human carotid plaques. Mol Imaging Biol 2012;14:277–285.

Richardson PD, Davies MJ, Born GV. Influence of plaque configuration and stress distribution on fissuring of coronary atherosclerotic plaques. Lancet 1989;334:941–944.

Sawada T, Shite J, Garcia-Garcia HM, Shinke T, Watanabe S, Otake H, Matsumoto D, Tanino Y, Ogasawara D, Kawamori H, Kato H, Miyoshi N, Yokoyama M, Serruys PW. Hirata K-i. Feasibility of combined use of intravascular ultrasound radiofrequency data analysis and optical coherence tomography for detecting thin-cap fibroatheroma. Eur Heart J 2008;29:1136–1146.

Schaar JA, Muller JE, Falk E, Virmani R, Fuster V, Serruys PW, Colombo A, Stefanadis C, Casscells WS, Moreno PR, Maseri A, van der Steen AFW. Terminology for high-risk and vulnerable coronary artery plaques. Eur Heart J 2004;25:1077–1082.

Schaar JA, van der Steen AF, Mastik F, Baldewsing RA, Serruys PW. Intravascular palpography for vulnerable plaque assessment. J Am Coll Cardiol 2006;47:C86–C91.

Schultz CJ, Serruys PW, van der Ent M, Ligthart J, Mastik F, Garg S, Muller JE, Wilder MA, van de Steen AF, Regar E. First-in-man clinical use of combined near-infrared spectroscopy and intravascular ultrasound: a potential key to predict distal embolization and no-reflow? J Am Coll Cardiol 2010;56:314.

Serruys PW, Garcia-Garcia HM, Buszman P, Erne P, Verheye S, Aschermann M, Duckers H, Bleie O, Dudek D, Botker HE, von Birgelen C, D'Amico D, Hutchinson T, Zambanini A, Mastik F,

van Es GA, van der Steen AF, Vince DG, Ganz P, Hamm CW, Wijns W, Zalewski A. Effects of the direct lipoprotein-associated phospholipase A(2) inhibitor darapladib on human coronary atherosclerotic plaque. Circulation 2008;118:1172–1182.

Sethuraman S, Amirian JH, Litovsky SH, Smalling RW, Emelianov SY. Spectroscopic intravascular photoacoustic imaging to differentiate atherosclerotic plaques. Opt Express 2008;16:3362–3367.

Shin ES, Garcia-Garcia HM, Ligthart JM, Witberg K, Schultz C, van der Steen AF, Serruys PW. In vivo findings of tissue characteristics using iMap IVUS and Virtual Histology IVUS. EuroIntervention 2011;6: 1017–1019. journal of EuroPCR in collaboration with the Working Group on Interventional Cardiology of the European Society of Cardiology.

Suh WM, Seto AH, Margey RJ, Cruz-Gonzalez I, Jang IK. Intravascular detection of the vulnerable plaque. Circ Cardiovasc Imaging 2011;4: 169–178.

Tearney GJ, Regar E, Akasaka T, Adriaenssens T, Barlis P, Bezerra HG, Bouma B, Bruining N, Cho J-M, Chowdhary S, Costa MA, de Silva R, Dijkstra J, Di Mario C, Dudeck D, Falk E, Feldman MD, Fitzgerald P, Garcia H, Gonzalo N, Granada JF, Guagliumi G, Holm NR, Honda Y, Ikeno F, Kawasaki M, Kochman J, Koltowski L, Kubo T, Kume T, Kyono H, Lam CCS, Lamouche G, Lee DP, Leon MB, Maehara A, Manfrini O, Mintz GS, Mizuno K, Morel M-A, Nadkarni S, Okura H, Otake H, Pietrasik A, Prati F, Räber L, Radu MD, Rieber J, Riga M, Rollins A, Rosenberg M, Sirbu V, Serruys PWJC, Shimada K, Shinke T, Shite J, Siegel E, Sonada S, Suter M, Takarada S, Tanaka A, Terashima M, Troels T, Uemura S, Ughi GJ, van Beusekom HMM, van der Steen AFW, van Es G-A, van Soest G, Virmani R, Waxman S, Weissman NJ, Weisz G. Consensus Standards for Acquisition, Measurement, and Reporting of Intravascular Optical Coherence Tomography Studies: A Report From the International Working Group for Intravascular Optical Coherence Tomography Standardization and Validation. J Am Coll Cardiol 2012;59:1058–1072.

Tearney GJ, Waxman S, Shishkov M, Vakoc BJ, Suter MJ, Freilich MI, Desjardins AE, Oh W-Y, Bartlett LA, Rosenberg M, Bouma BE. Three-dimensional coronary artery microscopy by intracoronary optical frequency domain imaging. J Am Coll Cardiol Img 2008;1: 752–761.

Tearney GJ, Yabushita H, Houser SL, Aretz HT, Jang I-K, Schlendorf KH, Kauffman CR, Shishkov M, Halpern EF, Bouma BE. Quantification of macrophage content in atherosclerotic plaques by optical coherence tomography. Circulation 2003;107:113–119.

Thim T, Hagensen MK, Wallace-Bradley D, Granada JF, Kaluza GL, Drouet L, Paaske WP, Botker HE, Falk E. Unreliable assessment of necrotic core by virtual histology intravascular ultrasound in porcine coronary artery disease. Circ Cardiovasc Imag 2010;3: 384–391.

Tromberg BJ, Shah N, Lanning R, Cerussi A, Espinoza J, Pham T, Svaasand L, Butler J. Non-invasive *in vivo* characterization of breast tumors using photon migration spectroscopy. Neoplasia 2000;2: 26–40.

Tsai CL, Chen JC, Wang WJ. Near-infrared absorption property of biological soft tissue constituents. J Med Biol Eng 2001;21:7–14.

Van Mieghem CA, McFadden EP, de Feyter PJ, Bruining N, Schaar JA, Mollet NR, Cademartiri F, Goedhart D, de Winter S, Granillo GR, Valgimigli M, Mastik F, van der Steen AF, van der Giessen WJ, Sianos G, Backx B, Morel MA, van Es GA, Zalewski A, Serruys PW. Noninvasive detection of subclinical coronary atherosclerosis coupled with assessment of changes in plaque characteristics using novel invasive imaging modalities: the Integrated Biomarker and Imaging Study (IBIS). J Am Coll Cardiol 2006;47: 1134–1142.

van Soest G, Goderie T, Regar E, Koljenovic S, van Leenders GLJH, Gonzalo N, van Noorden S, Okamura T, Bouma BE, Tearney GJ, Oosterhuis JW, Serruys PW, van der Steen AFW. Atherosclerotic tissue characterization in vivo by optical coherence tomography attenuation imaging. J Biomed Opt 2010;15:011105.

Van Veen RLP, Sterenborg HJCM, Pifferi A, Torricelli A, Cubeddu R. Determination of VIS- NIR absorption coefficients of mammalian fat, with time- and spatially resolved diffuse reflectance and transmission spectroscopy. OSA Biomed Opt Topical Meeting; 2004.

Virmani R, Kolodgie FD, Burke AP, Farb A, Schwartz SM. Lessons from sudden coronary death: A comprehensive morphological classification scheme for atherosclerotic lesions. Arterioscler Thromb Vasc Biol 2000;20:1262–1275.

Wang B, Yantsen E, Larson T, Karpiouk AB, Sethuraman S, Su JL, Sokolov K, Emelianov SY. Plasmonic intravascular photoacoustic imaging for detection of macrophages in atherosclerotic plaques. Nano Letters 2009;9:2212–2217.

Wang B, Su JL, Amirian J, Litovsky SH, Smalling R, Emelianov S. Detection of lipid in atherosclerotic vessels using ultrasound-guided spectroscopic intravascular photoacoustic imaging. Opt Express 2010a;18:4889–4897.

Wang B, Su JL, Karpiouk AB, Sokolov KV, Smalling RW, Emelianov SY. Intravascular Photoacoustic Imaging. IEEE J Quantum Electron 2010b;16:588–599.

Wang B, Emelianov S. Thermal intravascular photoacoustic imaging. Biomed Opt Express 2011;2:3072–3078.

Wang B, Karpiouk A, Yeager D, Amirian J, Litovsky S, Smalling R, Emelianov S. In vivo intravascular ultrasound-guided photoacoustic imaging of lipid in plaques using an animal model of atherosclerosis. Ultrasound Med Biol 2012a;38:2098–2103.

Wang B, Karpiouk A, Yeager D, Amirian J, Litovsky S, Smalling R, Emelianov S. Intravascular photoacoustic imaging of lipid in atherosclerotic plaques in the presence of luminal blood. Opt Lett 2012b; 37:1244–1246.

Wang P, Wang P, Wang HW, Cheng JX. Mapping lipid and collagen by multispectral photoacoustic imaging of chemical bond vibration. J Biomed Opt 2012c;17:96010.

Waxman S, Freilich MI, Suter MJ, Shishkov M, Bilazarian S, Virmani R, Bouma BE, Tearney GJ. A case of lipid core plaque progression and rupture at the edge of a coronary stent: Elucidating the mechanisms of drug-eluting stent failure. CircCardiovasc Interv 2010;3:193–196.

Waxman S, Ishibashi F, Muller JE. Detection and treatment of vulnerable plaques and vulnerable patients: Novel approaches to prevention of coronary events. Circulation 2006;114:2390–2411.

Yeager D, Karpiouk A, Wang B, Amirian J, Sokolov K, Smalling R, Emelianov S. Intravascular photoacoustic imaging of exogenously labeled atherosclerotic plaque through luminal blood. J Biomed Opt 2012;17:106016.

Zhang EZ, Beard PC. A miniature all-optical photoacoustic imaging probe. Proc SPIE 2011;78991:F-6.